

PAPER • OPEN ACCESS

Maxwellian Neutron Spectrum generation and Stellar Cross-Section measurements: measurement of the $^{197}\text{Au}(n, \frac{\gamma}{\text{SF}})$ MACS.

To cite this article: P Jiménez-Bonilla *et al* 2018 *J. Phys.: Conf. Ser.* **940** 012044

View the [article online](#) for updates and enhancements.



IOP | ebooks™

Bringing you innovative digital publishing with leading voices to create your essential collection of books in STEM research.

Start exploring the collection - download the first chapter of every title for free.

Maxwellian Neutron Spectrum generation and Stellar Cross-Section measurements: measurement of the $^{197}\text{Au}(n,\gamma)$ MACS.

P Jiménez-Bonilla^{1,3,*}, J Praena^{2,3}, J M Quesada¹

¹Atomic, Molecular and Nuclear Physics Department. University of Seville, Spain.

²Atomic, Molecular and Nuclear Physics Department. University of Granada, Spain.

³Centro Nacional de Aceleradores (US-JA-CSIC), Spain.

E-mail: jimenezbpablo@gmail.com

Abstract. Maxwellian-averaged cross-sections (MACS) are needed as an input for the models of stellar s- and r-processes nucleosynthesis. MACS can be obtained from activation measurements, irradiating a sample with the neutron field generated by the $^7\text{Li}(p,n)^7\text{Be}$ reaction at 1912 keV proton energy. At this energy, the neutron energy spectrum is close ($R^2 \leq 0.9$) to a Maxwellian one of $kT=25$ keV. However, it was shown that shaping the energy of the incident proton beam is possible to generate a neutron field with an energy spectrum much closer to a real Maxwellian ($R^2 > 0.995$), therefore avoiding or minimizing corrections in the MACS calculation. We show a preliminary result of an experiment performed at JRC-IRMM (Geel) to confirm our method. We have measured the MACS_{30} ($kT=30$ keV) of the $^{197}\text{Au}(n,\gamma)$ reaction, at CNA (Seville). We obtained 612 mb, in good agreement with the latest measurements.

1. Introduction

Neutron capture is the main process responsible for the nucleosynthesis of the major part of the elements beyond iron [1]. In the helium-burning phase in red giants stars, neutrons are produced via (α,n) reactions. These neutrons are quickly thermalized through elastic scattering, and their velocities are represented by a Maxwell-Boltzmann distribution (or Maxwellian in unit of energy). A temperature of $T=3.48 \cdot 10^6$ K, typical of He-burning in red giants stars, corresponds to a Maxwellian distribution with $kT=30$ keV. The Maxwellian-averaged cross-section (MACS) or stellar cross-section of the involved isotopes is a key parameter for modeling the stellar sites. The MACS is defined as the ratio between $\langle \sigma v \rangle$ (reaction rate per particle pair) and v_T (particle most probably thermal velocity for a temperature T). Its expression is showed in eq. 1.

$$\text{MACS} \equiv \langle \sigma \rangle = \langle \sigma v \rangle / v_T = \frac{2}{\sqrt{\pi}} \cdot \frac{1}{(kT)^2} \cdot \int_0^\infty \sigma(E) \cdot E \cdot e^{-\frac{E}{kT}} dE \quad . \quad (\text{Eq. 1})$$

MACS can be obtained by time-of-flight (TOF) and activation techniques. In case of activation, a neutron flux with an energy spectrum close to a Maxwellian at 25 keV (MACS_{25}) ($\approx 90\%$ area

* To whom any correspondence should be addressed.



overlapping) can be generated using the ${}^7\text{Li}(p,n){}^7\text{Be}$ near the threshold [2,3]. To obtain the MACS, the experimentally measured cross-section value must be corrected for spectrum difference. In addition to this, if the MACS₃₀ is needed an extrapolation from the MACS₂₅ is necessary. For both, correction and extrapolation, the $\sigma(E)$ knowledge or assumption is mandatory (including resonances). However, it was shown [4] that it's possible to generate a more realistic (>99% area overlapping) Maxwellian, avoiding $\sigma(E)$ assumption and minimizing the corrections.

2. Maxwellian Neutron Spectrum generation method: experiment and simulations.

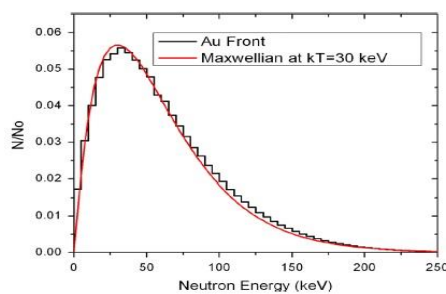


Figure 1. Simulated neutron spectrum for a GPD ($E_c=1851$ keV, FWHM=154 keV) on Li target.

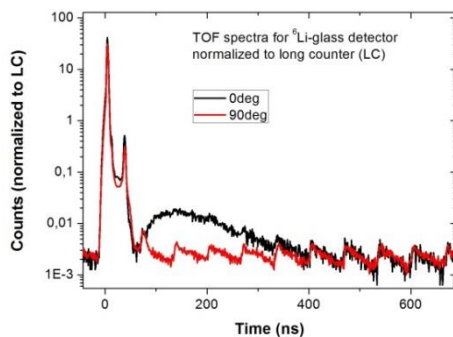


Figure 2. Normalized TOF spectra at 0° (black) and 90° (red).

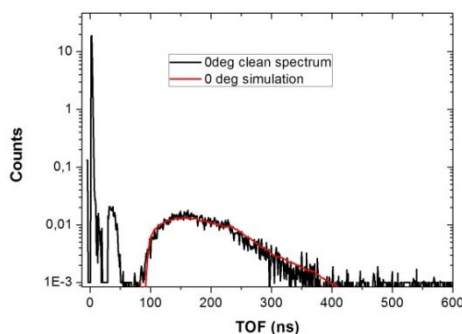


Figure 3. 0° TOF spectrum compared to SIMPRO procedure.

Our method for the production of Maxwellian Neutron Spectra is based on the shaping of the proton beam to a Gaussian-like distribution (GPD), introducing a foil degrader upstream of the lithium target [4]. The method was checked in [5,6]. Different combinations of proton energy and degrader material and thickness are suitable for generating Maxwellian-30. The GPDs were measured [5] and neutron spectra were obtained by means of analytical descriptions of the differential neutron yield in angle and energy of the ${}^7\text{Li}(p,n)$ reaction and Monte Carlo (MC) simulations of the neutron transport through the experimental setup (SIMPRO procedure) [5,6]. Fig.1 shows the neutron spectrum integrated over the Au sample (see Section 3) obtained with SIMPRO and compared to Maxwellian-30.

For an experimental confirmation of our method, we carried out an experiment at Van de Graaff at JRC-IRMM, briefly described here; more details will be given in a forthcoming paper. The proton beam energy was 3.7 MeV and the Al degrader 75 μm in thickness. We used the usual setup at IRMM for neutron spectrometry by time-of-flight (TOF) technique in this energy range that consisted of 625 kHz and 1-2 ns pulsed proton beam, with ${}^6\text{Li}$ -glass detectors located at 52 cm, more details of the electronic chain, detectors and materials can be found for similar experiments at IRMM [7].

Our experiment suffered from a contamination due to the proton beam halo at the accelerator source. At source, the beam was chopped by means of deflection plates sweeping it across a small aperture. When the proton beam was not passing across the aperture, a small part of the halo passed through it and was bunched. This effect is clearly shown in Fig.2, where the black line corresponds to TOF spectrum at 0° and red line at 90° (same detector). The highest peak in both spectra ($t=0-50$ ns) corresponds to prompt γ rays (so-called γ -flash) from reactions in the Al degrader, LiF (thick) target and Cu backing. Then, for higher times, neutrons are detected at 0° (from $\approx 80-400$ ns) and not at 90° . The lack of separation between the γ -peak and the neutron

“panettone” is due to the beam halo, producing a larger γ -peak in time than usual proton beam with no halo, and the high energy neutrons (up to 250 keV or 76 ns). Since the system was based on the pulse-height information of the detector, it was not possible to distinguish the γ -n contamination by combined pulse-shape analysis and TOF information. However, the neutron contamination is three orders of magnitude lower than the γ one, the same ratio than γ -flash and neutron “panettone” in Fig.1, therefore a reasonable clean TOF spectrum can be obtained by the subtraction of the 90° to 0° spectrum, both normalized to a long counter used as neutron monitoring. Fig.3 shows a clean 0° TOF spectrum compared to a time spectrum obtained with our SIMPRO procedure. In this case, SIMPRO consists of the inclusion in a MCNP file of the analytical description of the differential neutron yield in angle and energy of the $^7\text{Li}(p,n)$ for GPD ($E_c=1851$ keV, FWHM=154 keV). The MCNP file contains a detailed description of the ^6Li -glass detector at 52 cm from LiF target and Cu backing. Then, the time spectrum is obtained by means of Tally Time Card and a Tally Multiplier Card for the $^6\text{Li}(n,t)^4\text{He}$ reaction on the cell which contained the ^6Li -glass. The good agreement between the clean TOF spectrum and the SIMPRO suggests a preliminary experimental confirmation of our method and to continue cleaning all the measured angles.

3. $^{197}\text{Au}(n,\gamma)$ Stellar Cross Section measurement at $kT=30$ keV.

Gold is not a standard in the astrophysical energy range. However, it is commonly used as reference for neutron-capture cross-section measurements with $\text{MACS}_{30}=582\pm 9$ mb[8]. A large effort has been made to solve the MACS_{30} discrepancies between different experiments and techniques [8], in particular between TOF ones and the activation of [3]. Recently, we carried out the experiment of [3], quasi-Maxwellian, with Au flat sample and we obtained a value slightly higher, 626 ± 25 mb [9]. The main difference between MACS_{30} value in [3] and [9] is associated to the use of MC simulations for the neutron scattering correction. In [8] a new recommend value is given, 613 ± 7 mb. Here, we

measure the MACS_{30} with our method for Maxwellian-30 generation by means of GPD. Our measurement was carried out at the 3MV Tandem accelerator at CNA (Seville) with the same setup and procedure detailed in [5],[6] and [9]. Irradiation time was 210 min and measured time was 13h. A complete MCNPX simulation (gammas and neutron transport) of the setup and HPGe was carried out for the needed corrections [9]. Eq. 2, 3 and table 1 indicate the measured values and corrections. The obtained result for the $^{197}\text{Au}(n,\gamma)$ MACS_{30} is 612 ± 20 mb, very similar to our previous measurement [9] and the new recommend value 613 ± 7 mb [8].

Table 1. Measured values and corrections.

| | Value | ε (%) | |
|------------------------------|--------|-------------------|---------------------|
| C_{Au} | 64100 | 0.7 | Gamma counts. |
| C_{Be} | 545800 | 0.3 | Gamma counts. |
| $I_{\gamma\text{Au}}$ | 95.54 | 0.1 | Gamma intensity |
| $I_{\gamma\text{Be}}$ | 10.45 | 0.04 | Gamma intensity |
| N_{Au} | 6.4E-4 | 1.5 | Mass thickness. |
| $f_{d\text{Au}}$ | 0.1281 | 0.01 | Decay correction. |
| $f_{d\text{B}}$ | 0.0070 | 0.1 | Decay correction. |
| $\varepsilon_{\text{Be/Au}}$ | 0.80 | 1.9 | Gamma efficiency. |
| K_n | 1.75 | 1.3 | Neutron flux corr. |
| K_{macs} | 1.01 | 1.6 | Maxwellian correct. |

$$\text{MACS} = \frac{2}{\sqrt{\pi}} \cdot K_{\text{macs}} \cdot \sigma_{\text{exp}} \quad (\text{Eq. 2})$$

$$\sigma_{\text{exp}} = \frac{1}{N_{\text{Au}}} \cdot \frac{A_{\text{Au}}}{\Phi} = \frac{1}{N_{\text{Au}}} \cdot \frac{C_{\text{Au}}}{C_{\text{Be}}} \cdot \frac{[f_{d'} I_{\gamma'} \varepsilon]_{\text{Be}}}{[f_{d'} I_{\gamma'} \varepsilon]_{\text{Au}}} \cdot \frac{1}{K_n} \quad (\text{Eq.3})$$

References

- [1] E.M.Burbidge, G.R.Burbidge, W.A.Fowler, F.Hoyle, Rev.Mod.Phys.,v 29, n 4, 547-650 (1957).
- [2] H. Beer, F. Käppeler. Phys. Rev. C, vol. 21, n° 2, p.534–544 (1980).
- [3] W. Ratynski, F. Käppeler, Phys. Rev. C, 37 (1988) 595.
- [4] P. F. Mastinu, G. Martín-Hernández and J. Praena. Nucl. Inst. and Meth. A 601 (2009) 333-338.
- [5] J. Praena, P.F. Mastinu, M. Pignatari *et al.*, Nucl. Inst. and Meth. A, 727 1-6 (2013).
- [6] J. Praena, P.F. Mastinu, R. Capote *et al.*, Nuc. Data Sheets 120 (2014) 205–207.
- [7] G. Feinberg, M. Friedman, A. Krása, *et al.*, Phys. Rev. C, 85, 055810 (2012).
- [8] I. Dillmann, R.Plug, F.Käppeler, A.Mengoni, C.Heinz, M. Pignatari. “The new KADoNiS v1.0 and its influence on the weak s-process nucleosynthesis”. PoS (NIC XIII Conf.) 057 (2014)
- [9] P. Jiménez-Bonilla and J. Praena. Proceedings of Science PoS (NIC XIII) 102 (2014).